

Distribution of ^{56}Ni Yields of Type Ia Supernovae and its Implication for Progenitors *

Bo Wang^{1,2}, Xiang-Cun Meng^{1,2}, Xiao-Feng Wang^{3,4} and Zhan-Wen Han¹

¹ National Astronomical Observatories / Yunnan Observatory, Chinese Academy of Sciences, Kunming 650011; wangbo1129@hotmail.com

² Graduate School of Chinese Academy of Sciences, Beijing 100049

³ Tsinghua Center for Astrophysics (THCA) and Department of Physics, Tsinghua University, Beijing 100084

⁴ Astronomy Department, University of California at Berkeley, CA 94720, USA

Received 2007 April 13; accepted 2007 June 19

Abstract The amount of ^{56}Ni produced in Type Ia supernova (SN Ia) explosion is probably the most important physical parameter underlying the observed correlation of SN Ia luminosities with their light curves. Based on an empirical relation between the ^{56}Ni mass and the light curve parameter Δm_{15} , we obtained rough estimates of the ^{56}Ni mass for a large sample of nearby SNe Ia with the aim of exploring the diversity in SN Ia. We found that the derived ^{56}Ni masses for different SNe Ia could vary by a factor of ten (e.g., $M_{\text{Ni}} = 0.1 - 1.3 M_{\odot}$), which cannot be explained in terms of the standard Chandrasekhar-mass model (with a ^{56}Ni mass production of $0.4 - 0.8 M_{\odot}$). Different explosion and/or progenitor models are clearly required for various SNe Ia, in particular, for those extremely nickel-poor and nickel-rich producers. The nickel-rich (with $M_{\text{Ni}} > 0.8 M_{\odot}$) SNe Ia are very luminous and may have massive progenitors exceeding the Chandrasekhar-mass limit since extra progenitor fuel is required to produce more ^{56}Ni to power the light curve. This is also consistent with the finding that the intrinsically bright SNe Ia prefer to occur in stellar environments of young and massive stars. For example, 75% SNe Ia in spirals have $\Delta m_{15} < 1.2$ while this ratio is only 18% in E/SO galaxies. The nickel-poor SNe Ia (with $M_{\text{Ni}} < 0.2 M_{\odot}$) may invoke the sub-Chandrasekhar model, as most of them were found in early-type E/SO galaxies dominated by the older and low-mass stellar populations. This indicates that SNe Ia in spiral and E/SO galaxies have progenitors of different properties.

Key words: stars: evolution — supernovae : general — white dwarfs

1 INTRODUCTION

It is well known that Type Ia Supernovae (SNe Ia) are excellent cosmological distance indicators due to their high luminosity and remarkable uniformity. The results of the High-Z Supernova Search Team (Riess et al. 1998) and the Supernova Cosmology Project (Perlmutter et al. 1999) astonishingly showed that the expansion of the universe is accelerating. Although SNe Ia are very important objects in modern cosmology, several key issues related to the nature of their progenitor systems (Hachisu et al. 1996, 1999; Li & van den Heuvel 1997; Han & Podsiadlowski 2004; Meng et al. 2006) and the physics of the explosion mechanisms (Hillebrandt & Niemeyer 2000; Röpke & Hillebrandt 2005a) are still not well understood.

* Supported by the National Natural Science Foundation of China.

It is widely accepted that SNe Ia are thermonuclear explosions of carbon-oxygen (C-O) white dwarfs (WDs) accreting matter from their companions (for a review see Nomoto et al. 1997). The energy released from the burning till nuclear statistical equilibrium (NSE) completely destroys the C-O WD. The optical/IR light curves are powered by the radioactive decay of $^{56}\text{Ni} \rightarrow ^{56}\text{Co} \rightarrow ^{56}\text{Fe}$ (Colgate & Mckee 1969).

Over the last decades, it has been found that there exists spectroscopic diversity among SNe Ia. In an attempt to quantify the rate of spectroscopically peculiar SNe Ia in the existing observed sample, Branch et al. (1993) compiled a set of 84 SNe Ia and found that about 83% – 89% of the sample are normal (or sometimes “Branch normals”). According to Li et al. (2001), however, only $64\% \pm 12\%$ of observed SNe Ia are normal in a volume-limited search. The total rate of peculiar SNe Ia could be as high as $36\% \pm 9\%$. The rates are $16\% \pm 7\%$ and $20\% \pm 7\%$ for SN 1991bg-like events and SN 1991T-like objects, respectively. Moreover, some of the peculiar SNe Ia apparently deviate from the relation between the light-curve shape parameter Δm_{15} and the luminosity (e.g., Wang et al. 2006), which probably suggests that SN Ia luminosity is not a single parameter of the light curve shape. Note that Wang et al. (2005) presented a single post-maximum color parameter ΔC_{12} ($B - V$ color ~ 12 days after the B -band light maximum), which empirically describes almost the full range of the observed SN Ia luminosities and gives tighter correlations with the SN Ia luminosities, but the underpinning physics is still not understood. Stritzinger et al. (2006a) recently noticed that no explosion model has been proposed yet to successfully account for the factor of ten spanned by the range in the observed bolometric luminosity.

In this paper, we aim to understand the origin of the progenitors and explosion models with a large, well-observed sample of nearby SNe Ia. According to a simple empirical relation between the ^{56}Ni mass (M_{Ni}) and the decline rate parameter Δm_{15} , we can estimate the mass of radioactive material ^{56}Ni synthesized in SN Ia explosions. By studying the distribution of such a parameter for SNe Ia, we hope to obtain some clues to the SN Ia diversities. Moreover, we also investigate the correlation of SNe Ia distribution with their host galaxies, which might also set constraints on the SN Ia progenitors.

The paper is organized as follows. In Section 2, we provide a brief description of the observational data examined in this study. Section 3 shows the distribution of the decline rate parameter Δm_{15} , the relative radial distance r_{SN}/R_{25} and the derived ^{56}Ni mass. In particular, a simple empirical method is introduced and used to estimate the ^{56}Ni mass for a large number of well-observed SNe Ia. A discussion and conclusions are then given in Section 4.

2 DATA

In this paper, we consider a sample of 111 well-observed nearby SNe Ia with $Z < 0.1$, of these 109 were compiled by Wang et al. (2006) (see tables 1 and 2 in their work), and SNe 2002cs and 2002dj are from unpublished KAIT SN database. The sample (excepting SNe 1937C, 1972E and 1974G) includes only SNe with CCD measurements and those observed not later than 8 days after the B -band light maximum and with more than five photometric points. A large fraction of these observations were obtained by the earlier Calan/Tololo SN survey, the CfA I/II SN monitoring campaign, and the Las Campanas/CTIO observing campaign.

The sample contains two important parameters (i.e., Δm_{15} and r_{SN}/R_{25}). The decline rate parameter Δm_{15} was defined by Phillips (1993) as the amount in magnitudes that the B -band light curve decays in the first 15 days after maximum light, and the decline rate was corrected for a small reddening effect (Phillips et al. 1999); r_{SN}/R_{25} is the de-projected galactocentric distance of the SNe in their respective host galaxies in units of the galaxy radius R_{25} , where r_{SN} is the de-projected radial distance of the SN Ia from the galactic center and R_{25} the apparent semimajor axes of the SN host galaxy isophote having $\mu_B = 25.0 \text{ mag arcsec}^{-2}$. The 111 well-observed sample contains 90 spectroscopically normal SNe Ia, 13 SN 1991T-like objects, six SN 1991bg-like events and two truly peculiar SNe Ia, SNe 2001ay and 2002cx. The 111 sample can be divided into four groups by the morphological type of their host galaxies: 77 are in spiral galaxies, 28 in E/S0 galaxies, two (SNe 1972E and 2000fa) in irregular galaxies, and four (SNe 1992bl, 1999aw, 1999ej and 2002cx) in galaxies of uncertain or intermediate types. Again, the sample of 111 contains 98 SNe Ia with relative radial distances while the remainder are uncertain. Out of the 98 SNe Ia with known distances, 26 are from E/S0 galaxies, 70 from spiral galaxies, one (SN 1992bl) from a S0/a galaxy and one (SN 2000fa) from an irregular galaxy.

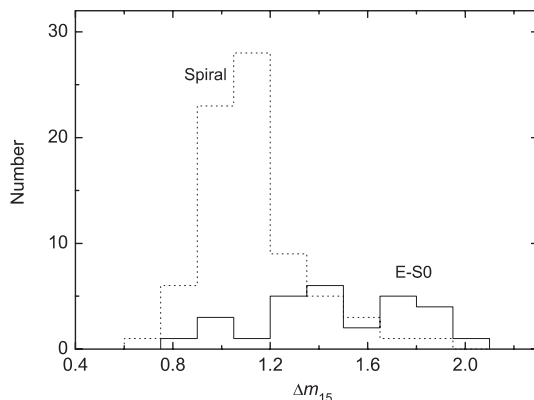


Fig. 1 Distribution of Δm_{15} for 28 SNe Ia in E/S0 galaxies (solid line) and 77 in spiral galaxies (dotted line).

3 ANALYSIS AND RESULTS

In this section we investigate the distributions of Δm_{15} and the derived ^{56}Ni mass versus r_{SN}/R_{25} . In particular, we provide a short overview of the method to estimate the ^{56}Ni masses for a large number of well-observed SNe Ia.

3.1 Distribution of Δm_{15}

Using optical light curves of SNe Ia, Phillips (1993), Hamuy et al. (1996a) and Phillips et al. (1999) established a relationship between the absolute magnitude at B -band light maximum and the initial decline rate of the light curve. The characteristic parameter is Δm_{15} . When Δm_{15} is properly corrected for, the SNe Ia prove to be a high precision distance indicator, yielding relative distances with uncertainties $\sim 7\%–10\%$ (Hamuy et al. 1996b). Kasen & Woosley (2007) confirmed that the brighter SNe Ia have broader B -band light curves with smaller decline rates around optical maxima than the dimmer SNe Ia. Moreover, the determination of the decline rate parameter Δm_{15} is available for a large number of objects. By analyzing Δm_{15} , it is possible for us to peer into some intrinsic properties of SNe Ia, because it is basically independent of distance and reddening.

Hamuy et al. (1995, 1996a) first noticed that brighter (also smaller Δm_{15}) SNe Ia are preferentially located in late-type galaxies for the nearby sample of SN Ia (see also Gallagher et al. 2005). In Figure 1, we show the distribution of Δm_{15} for spiral and E/S0 galaxies, where the mean error for Δm_{15} is 0.07. It is obvious that the distribution of Δm_{15} is different in spiral and E/S0 galaxies. A K-S test shows that the probability of these two distributions coming from the same population is as low as $P = 3.3 \times 10^{-7}$ (see also Altavilla et al. 2004; Della Valle et al. 2005 for similar argument). Although both SNe Ia in spiral and E/S0 galaxies show a wide range of Δm_{15} , the fraction with $\Delta m_{15} < 1.2$ is 75% in spirals and only 18% in E/S0 galaxies. The fact that faster decliners (i.e., fainter SNe Ia) dominate in E/S0 galaxies is apparently related to the age of the progenitors since E/S0 galaxies are believed to have older low-mass stars. Recently, Sullivan et al. (2006) demonstrated that the stretch factor of SNe Ia (another form of Δm_{15}) in low- and high-redshift spiral galaxies bears the same distribution at a confidence level of 95%, while the distributions in elliptical galaxies are different as the faster decliners (also the fainter SNe Ia) are usually seldom observed at high redshift probably due to the selection effect and/or the SN evolution effect. Since the decline rate Δm_{15} is tightly correlated with the stretch factor s , this difference found in elliptical galaxies holds true for Δm_{15} .

Figure 2 shows the distribution of Δm_{15} for different types of SNe Ia. Compared with normal SNe Ia, SN 1991T-like events have a flatter decline rate of 0.95 ± 0.10 while SN 1991bg-like objects have a much faster decline rate of 1.90 ± 0.10 . In the figure SNe 2001ay and 2002cx are truly peculiar events. SN 2001ay has the slowest decline rate in our sample, and Howell & Nugent (2004) suggested that SN 2001ay is an SN Ia with the broadest light curve. Li et al. (2003) noted that SN 2002cx has a pre-maximum spectrum like SN

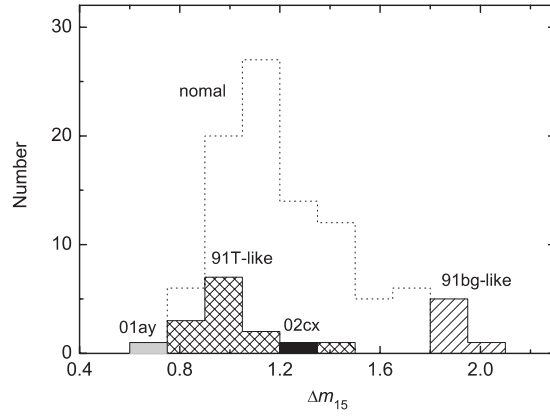


Fig. 2 Distribution of Δm_{15} for different SN Ia types. The dotted line shows the distribution of 90 normal SNe Ia. The cross-hatched area and the simply shaded area are for 13 SN 1991T-like events and six SN 1991bg-like objects, respectively. The gray-color area and the black area show SNe 2001ay and 2002cx, respectively.

1991T (the classical hot SN Ia), a luminosity like SN 1991bg (the classic subluminous event), a slow late-time decline, and unidentified spectral lines (which is probably not an SN Ia as it showed a spectroscopic feature extremely similar to those in some faint type II-P SNe at nebular phase, private communication with Dr. Weidong Li).

3.2 Distribution of r_{SN}/R_{25}

The distribution of SNe Ia in host galaxies can provide important clues to their progenitors and also give constraints on the explosion models. In Figure 3, the decline rate Δm_{15} is plotted against the normalized radial distance r_{SN}/R_{25} . The filled circles mark the 26 SNe Ia in E/S0 galaxies, and the open circles, the 70 SNe Ia in spirals, with the observational error bars shown. In the figure SN 2002cs is a slow decliner (with $\Delta m_{15}=1.00$) in the elliptical galaxy NGC 6702, and SN 2002dj is another slow decliner (with $\Delta m_{15}=1.05$) in the elliptical galaxy NGC 5018. Moreover, SN 1998es is an SN 1991T-like object in a lenticular galaxy. Its host galaxy NGC 632 has a nuclear starburst with a diameter of 18 kpc, and the position of SN 1998es is projected near the edge of the star-forming region (Jha et al. 1998).

Figure 4 shows the distribution of the normalized radial distance r_{SN}/R_{25} . Wang (2002) first noticed that SNe Ia might be more centrally concentrated in spiral galaxies than in E/S0 galaxies. In our study, the fraction of SNe Ia in E/S0 galaxies located in the $r_{\text{SN}}/R_{25} > 1.0$ region is about 23%, while this fraction is only 4% for the SNe Ia in spirals. In other words, SNe Ia in spiral galaxies could be more concentrated towards the optical R_{25} radius of their host galaxies than in E/S0 galaxies. A K-S test shows there is only a 33% probability that the ancestors of SNe Ia in the E/S0 and the spiral galaxies have the same radial distribution. Furthermore, the plot displays a deficiency of SNe Ia in the central $r_{\text{SN}}/R_{25} \leq 0.2$ region. The data on the SNe Ia radial distribution closer to center the galaxies can be affected by absorption (Windhorst et al. 2002). Note that this effect on the SNe Ia distribution closer to the center of the galaxies may be more serious in spiral galaxies with abundant gas and dust. Therefore, SNe Ia in spiral galaxies may be more centrally located than the above number suggests.

3.3 $M_{\text{Ni}} - \Delta m_{15}$ Relation

The mass of ^{56}Ni produced during an SN Ia explosion is the primary physical parameter determining the luminosity of the event. One simple method to estimate the synthesized ^{56}Ni mass is a detailed calculation on the assumption that the maximum luminosity of an SN Ia is proportional to the instantaneous rate of radioactive decay (Arnett 1982; Arnett et al. 1985; Branch 1992). Thus the implied bolometric luminosity at light maximum (the luminosity integrated from ultraviolet to infrared) can be expressed as

$$L_{\text{bol}} = \alpha \dot{S}(t_{\text{R}}) M_{\text{Ni}}, \quad (1)$$

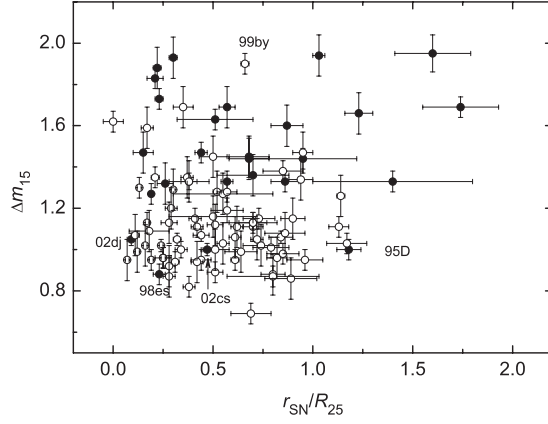


Fig. 3 Plotted Δm_{15} against the normalized radial distance r_{SN}/R_{25} . The filled circles show 26 SNe Ia in E/S0 galaxies. The open circles represent 70 SNe Ia in spiral galaxies.

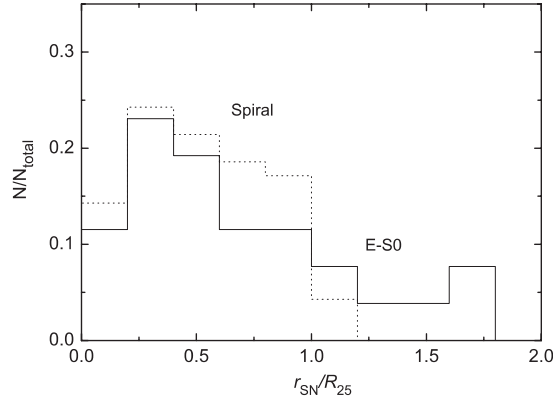


Fig. 4 Distribution of the normalized radial distance r_{SN}/R_{25} for SNe Ia in E/S0 galaxies (solid line) and in spiral galaxies (dotted line).

where M_{Ni} is the total mass of ^{56}Ni produced in the explosion, α the ratio of bolometric to radioactivity luminosity, and $\dot{S}(r_{\text{R}})$ the radioactivity luminosity per solar mass of ^{56}Ni from its decay to ^{56}Co and the subsequent decay to ^{56}Fe (e.g., Nadyozhin 1994):

$$\dot{S} = 6.45 \times 10^{43} e^{-t_{\text{R}}/8.8} + 1.45 \times 10^{43} e^{-t_{\text{R}}/111.3} \text{ erg s}^{-1} M_{\odot}^{-1}, \quad (2)$$

where t_{R} is the rise time in days from the SN explosion to the light maximum. A typical rise time of 19 ± 2 days is assumed for SNe Ia in our analysis (cf., Branch 1992).

From the analytic solutions for the early-epoch SN Ia light curves, Arnett (1982) found that α should be 1 exactly. On the other hand, according to an early survey of SN Ia lightcurve calculations, Branch (1992) found that α is slightly larger than unity. He concluded $\alpha = 1.2 \pm 0.2$ and noted that the value of α is independent of the rise time. We assume $\alpha = 1$ in our analysis because the nickel produced above the photosphere may not make significant contribution to the luminosity (e.g., Nugent et al. 1995). Stritzinger & Leibundgut (2005) noted that light curves of two 3-D SNe Ia explosion models recently synthesized by the MPA group are consistent with $\alpha = 1$. Using Arnett's rule ($\alpha = 1.0$) which states that the maximum luminosity of an SN Ia is equal to the instantaneous energy deposition rate from the radioactive decays within the expanding ejecta (Arnett 1982; Arnett et al. 1985), and assuming a rise time to bolometric maximum of

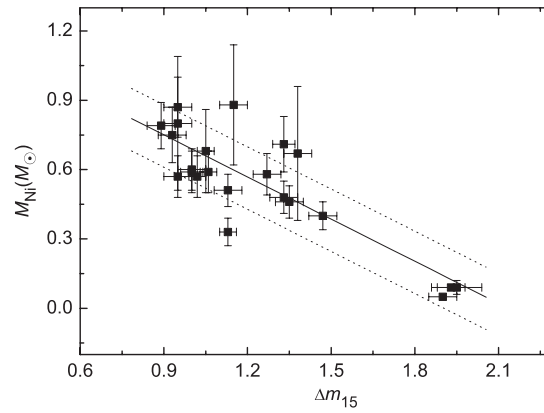


Fig. 5 ^{56}Ni mass derived from maximum luminosity vs. Δm_{15} for 22 well-observed SNe Ia. The solid line marks the least squares fit. The dotted lines correspond to a vertical deviation of $0.13 M_{\odot}$ (i.e., a quoted dispersion “ σ ”) about the solid line. Note that the solid line is similar to the relation obtained by Phillips (1993), Phillips et al. (1999).

19 days, one can derive from Equations (1) and (2) a simple formula for the maximum luminosity of an SN Ia (e.g., Stritzinger & Leibundgut 2005):

$$L_{\text{max}} = (2.0 \pm 0.3) \times 10^{43} \left(\frac{M_{\text{Ni}}}{M_{\odot}} \right) \text{ erg s}^{-1}. \quad (3)$$

The uncertainty of the derived ^{56}Ni mass is primarily determined by the errors in the adopted bolometric rise time and the transformation efficiency of the trapped γ energy.

It is generally believed that the ^{56}Ni mass can be better measured by the bolometric light curves constructed from the light curves in the ultraviolet, optical and infrared wavelengths. However, only a few SNe Ia have good observations covering from UV to IR , which could be used as a training sample for ^{56}Ni mass determination of other SNe Ia. In Figure 5, the ^{56}Ni masses derived from 22 well-observed SNe Ia with $UBVRI$ and infrared light curves are plotted vs. Δm_{15} . For consistency in the Δm_{15} determinations, Δm_{15} values of the 22 training SNe Ia are taken from table 1 in Wang et al. (2006). Of the 22 SNe Ia with ^{56}Ni estimates, 17 are from table 2 in Stritzinger et al. (2006b) and five (SNe 1995E, 1998aq, 1998de, 1999ac and 1999dq) from table 1 in Stritzinger et al. (2006a). To derive the ^{56}Ni masses Stritzinger et al. (2006 a, b) made use of Equation (3). In Figure 5, the solid line corresponding to a least squares fit of the data yields the following zero points and dispersion:

$$M_{\text{Ni}} = (-0.61 \pm 0.09)\Delta m_{15} + (1.30 \pm 0.11), \quad \sigma = 0.13, \quad N = 22, \quad (4)$$

where the quoted dispersion “ σ ” is the simple root mean square (rms) deviation of the points about the fit. Our fitting result is very similar to that of Mazzali et al. (2007). Note that the least square fit line is similar to the Phillips M_B - Δm_{15} relation (Phillips 1993; Phillips et al. 1999). A vertical deviation of $0.13 M_{\odot}$ (dotted lines) about the solid line is also shown. It is suggested that the maximum luminosity of an SN Ia (Δm_{15}) could be a direct consequence of the ^{56}Ni mass via modelling the light curves of SNe Ia (Arnett 1982; Cappellaro et al. 1997; Mazzali et al. 2001; Kasen 2006). The correlation between the ^{56}Ni mass and Δm_{15} shown in Figure 5 may be taken as observational evidence for this assumption.

3.4 Distribution of ^{56}Ni Masses

The amount of ^{56}Ni synthesized from burning to nuclear statistical equilibrium (NSE) in SN Ia explosions is probably the most important physical parameter underlying the observed correlation of SN Ia luminosities with their light curves. With the ^{56}Ni mass one can directly study the most sensitive part of the explosion

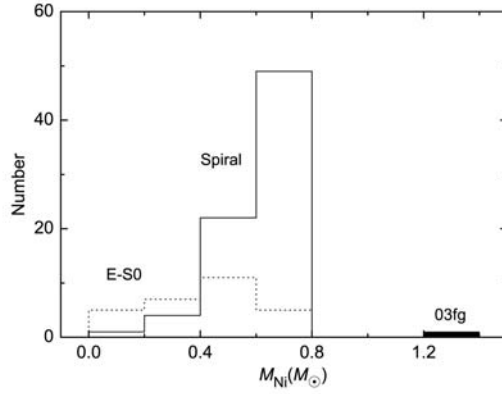


Fig. 6 Distribution of the ^{56}Ni mass for 28 SNe Ia in E/S0 galaxies (dotted line) and 76 in spiral galaxies (solid line) excepting the truly peculiar SN 2001ay. The black area represents SN 2003fg.

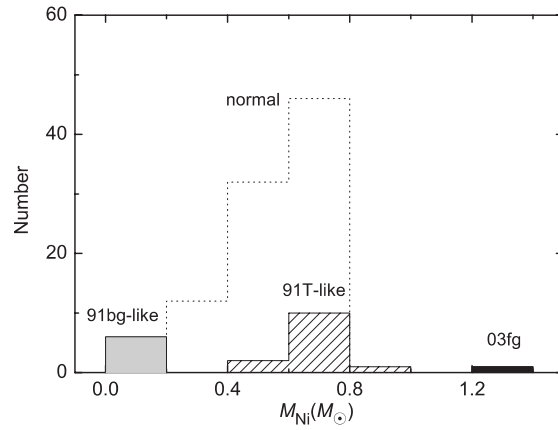


Fig. 7 Distribution of the ^{56}Ni mass for different SN Ia types. The dotted line is for the 90 normal SNe Ia. The gray-color area and the single shaded area are for six SN 1991bg-like events and 13 SN 1991T-like objects, respectively. The black area represents SN 2003fg.

and provide constraints on the explosion mechanisms (see the review in Leibundgut 2000). Here, according to the empirical relation between the ^{56}Ni mass and Δm_{15} , i.e., Equation (4), we can estimate the ^{56}Ni masses and give the distribution of the ^{56}Ni mass for a large number of SNe Ia (see Figs. 6 and 7).

As shown in Figures 6 and 7, the ^{56}Ni mass synthesized in SN Ia explosions varies from 0.1 to $1.3 M_{\odot}$, with mean error $0.17 M_{\odot}$. Figure 6 displays the distribution of the ^{56}Ni mass for SNe Ia in spiral and E/S0 galaxies, the black area represents SN 2003fg. To produce SN 2003fg's unusual luminosity, Howell et al. (2006) calculated, using Equation (1), ^{56}Ni mass, $M_{\text{Ni}} = 1.29 \pm 0.07 M_{\odot}$, a value that was further confirmed by Jeffery et al. (2006). In Figure 7 we show the distribution of the ^{56}Ni mass for different SN Ia types, and it is indicated that different SN Ia types (i.e., normal SNe Ia, SN 1991bg-like events and SN 1991T-like objects) require the existence of a range in the ^{56}Ni masses in SN Ia explosions.

4 DISCUSSION AND CONCLUSIONS

As we know from Section 3.1, the brighter SNe Ia prefer to occur in spiral galaxies and the fainter ones, in E/S0 galaxies. However, SNe 2002cs and 2002dj are slow decliners in elliptical galaxies. This contradicts

with previous conclusion that elliptical galaxies produce only fainter SNe Ia. These two cases probably suggest that the age may not be the exclusive factor underlying SN Ia diversities. Moreover, SN 1998es is a slow decliner in a nuclear starburst galaxy, which can probably be taken as an instance of brighter events occurring in systems with ongoing star formation (Sullivan et al. 2006). Figure 4 shows that SNe Ia might be more concentrated towards the optical R_{25} radius of their host galaxies in spirals than in E/S0 galaxies. This suggests that SNe Ia in spiral and E/S0 galaxies might have different progenitor properties.

There is increasing evidence that a single parameter (Δm_{15}) cannot account for the diversity in SN Ia (e.g., Benetti et al. 2004). As shown in Figure 5, there is a relatively large scatter $\sim 0.13 M_{\odot}$ in the ^{56}Ni mass — Δm_{15} relation. The dispersion may be partly due to uncertainties in the distance and reddening adopted in the calculations, but an intrinsic dispersion cannot be ruled out. Although it is believed that the ^{56}Ni mass in SN Ia explosions is the dominant physical parameter affecting both the brightness and light curve shape (or Δm_{15}), Woosley et al. (2006) proposed that some parameters other than M_{Ni} also affect the light curves to some extent, such as the total burned mass, the stable iron mass and the degree of direct ^{56}Ni mixing. However, since the empirical $M_{\text{Ni}} - \Delta m_{15}$ relation is similar to the Phillips $M_B - \Delta m_{15}$ relation and the larger sample used in the analysis helps to reduce the effect of random error, it is reliable to use the relation to roughly estimate the ^{56}Ni mass.

Based on the distribution of ^{56}Ni masses above, it is shown that ^{56}Ni mass varies by at least a factor of ten (e.g., $M_{\text{Ni}} = 0.1 - 1.3 M_{\odot}$). The explosions of SNe Ia might produce a range in the amount of ^{56}Ni synthesized from $\sim 0.1 M_{\odot}$ associated with the subluminal objects to $\sim 1.3 M_{\odot}$ for the most luminous events. The wide distribution of ^{56}Ni masses raises the question as to what physical mechanism(s) can account for this dispersion. During the past years, a number of potential parameters in the Chandrasekhar-mass deflagration scenario were investigated to answer this question, e.g., C-O ratio, overall metallicity and central density. However, 3D simulations by Röpke & Hillebrandt (2004) indicated that different C-O ratios have a negligible effect on the amount of ^{56}Ni produced. Also Röpke et al. (2005b) showed that there exists a $\sim 20\%$ change in the resulting ^{56}Ni masses via altering the metallicity, which is consistent with the analytic prediction of Timmes et al. (2003). Moreover, it has been shown that changing the central density of the white dwarf does influence the robustness of the explosion. Again, Stritzinger et al. (2006a) suggested that it is unrealistic that any one of these parameters, or even a combination of all three, can account for a factor of ten range in the ^{56}Ni mass.

Besides these parameters, the explosion mechanism itself is more likely to influence the ^{56}Ni masses synthesized in SN Ia explosions (see Stritzinger & Leibundgut 2005). The standard Chandrasekhar-mass model is the most popular explosion scenario for SNe Ia. However, different Chandrasekhar-mass models can produce different amount of ^{56}Ni which is usually in the range of $0.4 - 0.8 M_{\odot}$ (e.g., Mazzali et al. 2001), thus it is an observational fact that a single class of Chandrasekhar-mass model cannot account for the explosion properties of all the SNe Ia. Recently, Mazzali et al. (2007) accomplished a systematic spectral analysis of a large sample of well-observed SNe Ia and mapped the velocity distribution of the main products of nuclear burning in SN Ia explosions. They indicated that a single explosion scenario, possibly a delayed detonation (DD) of Chandrasekhar-mass model, may explain most SNe Ia. From the distribution of the ^{56}Ni mass displayed above, one can find that the ^{56}Ni mass falls mostly in the range of $0.4 - 0.8 M_{\odot}$, thus we suggest that a Chandrasekhar-mass model might account for normal SNe Ia which have the ^{56}Ni masses from $0.4 M_{\odot}$ to $0.8 M_{\odot}$. Moreover, sub-Chandrasekhar WDs are plausible candidates for the subluminal objects. We note that one appealing advantage offered by a sub-Chandrasekhar model is the ability to obtain the progenitor statistics predicted by population synthesis calculations (Livio 2000). In addition, the sub-Chandrasekhar model can easily explain the observed diversity of SNe Ia by a one parameter sequence in terms of the WD mass (Ruiz-Lapuente et al. 1995), and we also suggested flexible progenitors for SN 1991bg-like events with $M_{\text{Ni}} < 0.2 M_{\odot}$ (Cappellaro et al. 1997; Stritzinger et al. 2006a, b). However, it must be noted that the sub-Chandrasekhar model has difficulty in matching the observed light curves and spectroscopy (e.g., Höflich & Khokhlov 1996).

As shown in Figure 7, the ^{56}Ni mass of SN 2003fg exceeds others remarkably. Hillebrandt et al. (2007) argued that a lop-sided explosion of a Chandrasekhar-mass WD could provide a better explanation for SN 2003fg. They suggested that such objects must be rare, since both a moderately high ^{56}Ni mass ($\geq 0.9 M_{\odot}$) and a rather special viewing direction are rare. However, it is commonly believed that SN 2003fg could be from a super-Chandrasekhar WD explosion (e.g., Uenishi et al. 2003; Yoon & Langer 2005; Howell et al.

2006; Jeffery et al. 2006). It is proposed that the influence of rotation of the accreting WDs may cause the mass to exceed $1.4 M_{\odot}$. Mazzali et al. (2007) also noted that some extremely luminous SNe Ia may come from very rapidly rotating WDs whose mass exceeds the Chandrasekhar mass, but these are rare.

In summary, the wide distribution of the ^{56}Ni mass suggests that there are probably multiple origins of SN Ia explosion and/or progenitor systems. We argue that sub-Chandrasekhar WDs could be the progenitors of some extremely nickel-poor SNe Ia (with $M_{\text{Ni}} < 0.2 M_{\odot}$), and that super-Chandrasekhar WDs the progenitors of some rare nickel-rich SNe Ia (with $M_{\text{Ni}} > 0.8 M_{\odot}$). The Chandrasekhar-mass model remains the main scenario for SN Ia explosions with a range in ^{56}Ni masses from $0.4 M_{\odot}$ to $0.8 M_{\odot}$. To set further constraints on SN Ia explosion/progenitor models, large samples of SNe Ia with well-observed light curves and spectroscopy in nearby galaxies are required to establish the connection of SN Ia properties with the stellar environments of their host galaxies.

Acknowledgements We acknowledge Dr. Weidong Li for providing the SNe 2002cs and 2002dj parameters before publication. We also thank the referee for careful reading of the paper and valuable suggestions. This work is supported by the National Natural Science Foundation of China (grant Nos. 10433030, 10521001 and 10673007), the Foundation of the Chinese Academy of Sciences (No. KJ CX2-SW-T06), and Basic Research Funding at Tsinghua University (JCqn2005036).

References

- Altavilla G., Fiorentino G., Marconi M. et al., 2004, MNRAS, 349, 1344
 Arnett W. D., 1982, ApJ, 253, 785
 Arnett W. D., Branch D., Wheeler J. C., 1985, Nature, 314, 337
 Benetti S., Meikle P., Stehle M. et al., 2004, MNRAS, 348, 261
 Branch D., 1992, ApJ, 392, 35
 Branch D., Fisher A., Nugent P., 1993, AJ, 106, 2383
 Cappellaro E., Mazzali P. A., Benetti S. et al., 1997, A&A, 328, 203
 Colgate S. A., Mckee C., 1969, ApJ, 157, 623
 Della Valle M., Panagia N., Padovani P. et al., 2005, ApJ, 629, 750
 Gallagher J. S., Garnavich P. M., Berlind P. et al., 2005, ApJ, 634, 210
 Hachisu I., Kato M., Nomoto K., 1996, ApJ, 470, L97
 Hachisu I., Kato M., Nomoto K., 1999, ApJ, 522, 487
 Hamuy M., Phillips M. M., Maza J. et al., 1995, AJ, 109, 1
 Hamuy M., Phillips M. M., Suntzeff N. B. et al., 1996a, AJ, 112, 2391
 Hamuy M., Phillips M. M., Suntzeff N. B. et al., 1996b, AJ, 112, 2398
 Han Z., Podsiadlowski Ph., 2004, MNRAS, 350, 1301
 Hillebrandt W., Niemeyer J. C., 2000, ARA&A, 38, 191
 Hillebrandt W., Sim S. A., Röpke F. K., 2007, A&A, 465, L17
 Höflich P., Khokhlov A., 1996, ApJ, 457, 500
 Howell D. A., Nugent P., 2004, In: P. Höflich et al., eds., in Cosmic Explosions in Three Dimensions: Asymmetries in Supernovae and Gamma-Ray Bursts, Cambridge: Cambridge University Press, P.151
 Howell D. A., Sullivan M., Nugent P. E. et al., 2006, Nature, 443, 308
 Jeffery D. J., Branch D., Baron E., 2006, in press (astro-ph/0609804)
 Jha S., Garnavich P., Challis P. et al., 1998, IAU Circ., 7054
 Kasen D., 2006, ApJ, 649, 939
 Kasen D., Woosley S. E., 2007, ApJ, 656, 661
 Leibundgut B., 2000, A&ARv, 10, 179
 Li W. D., Filippenko A. V., Treffers R. R. et al., 2001, ApJ, 546, 734
 Li W. D., Filippenko A. V., Chornock R. et al., 2003, PASP, 115, 453
 Li X. D., van den Heuvel E. P. J., 1997, A&A, 322, L9
 Livio M., 2000, in press (astro-ph/0005344)
 Mazzali P. A., Nomoto K., Cappellaro E. et al., 2001, ApJ, 547, 988
 Mazzali P. A., Röpke F. K., Benetti S. et al., 2007, Science, 315, 825
 Meng X., Chen X., Tout C. A., Han Z., 2006, Chin. J. Astron. Astrophys. (ChJAA), 6, 461

- Nadyozhin D. K., 1994, *ApJS*, 92, 527
Nomoto K., Iwamoto K., Kishimoto N., 1997, *Science*, 276, 1378
Nugent P., Branch D., Baron E. et al., 1995, *PhRvL*, 75, 394
Perlmutter S., Aldering G., Goldhaber G. et al., 1999, *ApJ*, 517, 565
Phillips M. M., 1993, *ApJ*, 413, L105
Phillips M. M., Lira P., Suntzeff N. B. et al., 1999, *AJ*, 118, 1766
Riess A. G., Filippenko A. V., Challis P. et al., 1998, *AJ*, 116, 1009
Röpke F. K., Hillebrandt W., 2004, *A&A*, 420, L1
Röpke F. K., Hillebrandt W., 2005a, *A&A*, 431, 635
Röpke F. K., Gieseler M., Hillebrandt W., 2005b, *ASPC*, 342, 397
Ruiz-Lapuente P., Burkert A., Canal R., 1995, *ApJ*, 447, L69
Stritzinger M., Leibundgut B., 2005, *A&A*, 431, 423
Stritzinger M., Leibundgut B., Walch S. et al., 2006a, *A&A*, 450, 241
Stritzinger M., Mazzali P. A., Sollerman J. et al., 2006b, *A&A*, 460, 793
Sullivan M., Le Borgne D., Pritchett C. J. et al., 2006, *ApJ*, 648, 868
Timmes F. X., Brown E. F., Truran J. W., 2003, *ApJ*, 590, L83
Uenishi T., Nomoto K., Hachisu I., 2003, *ApJ*, 595, 1094
Wang X. F., 2002, PhD Thesis, Beijing Normal University
Wang X. F., Wang L. F., Zhou X. et al., 2005, *ApJ*, 620, L87
Wang X. F., Wang L. F., Pain R. et al., 2006, *ApJ*, 645, 488
Windhorst R. A., Taylor V. A., Jansen R. A. et al., 2002, *ApJS*, 143, 113
Woosley S. E., Kasen D., Blinnikov S. et al., 2006, in press (astro-ph/0609562)
Yoon S.-C., Langer N., 2005, *A&A*, 435, 967